

C H A P T E R V

EXPERIMENTAL DETERMINATION OF THE ELASTIC CONSTANT K_{13} OF A NEMATIC LIQUID CRYSTAL

5.1 INTRODUCTION

As we have seen in the earlier chapters, surface anchoring plays an important role in studying various physical properties of liquid crystals. For example, a homeotropic anchoring at the surfaces is essential to obtain the order parameters using the method described in Chapter III. On the other hand, a practically zero anchoring energy is necessary to observe the 'Lehmann rotation' phenomenon as described in Chapter IV. It is also known that a surface with a weak anchoring is required in some manifestations of the flexoelectric effects (Madhusudana and Durand 1985). The alignment of liquid crystalline samples is influenced by the strength of the anchoring at the surfaces. As we shall discuss in this Chapter a weak anchoring at the surfaces makes it possible to determine a new elastic constant in nematics. The main theme of this thesis has been physical studies on liquid crystalline mixtures. However in this chapter we make a departure and report some preliminary measurements on the value of the elastic constant K_{13} for a pure compound.

We now briefly recall the theory of elasticity of uniaxial

nematic liquid crystals. As mentioned in Chapter I the elastic properties of liquid crystals are generally described by an energy density function which depends on local deformations (Oseen 1933, Frank 1958). The elastic free energy density of a nematic which is characterised by an apolar director consists of quadratic terms of the curvature components describing splay, bend and twist of the director, associated with the elastic constants K_{11} , K_{22} and K_{33} respectively. Frank's formulation contains an additional term of the same order associated with $(K_{22} + K_{24})$. Nehring and Saupe (1971) argued that another term which is a second derivative of the curvature components associated with the elastic constant K_{13} should also be taken into account as it is of the same order. We now summarise the derivation of the free energy density including the K_{13} term, following the formalism of Nehring and Saupe.

5.2 DERIVATION OF THE FREE ENERGY DENSITY

As defined before (Chapter I) $\vec{n}(\mathbf{r})$ which represents the preferred orientation at a point is assumed to vary slowly and continuously with position. A local system of Cartesian coordinates x, y, z can be introduced at any point with the z -axis along \vec{n} at that point. The x -axis is chosen arbitrarily perpendicular to z , and the y axis is chosen to be perpendicular to x such that x, y, z form a right handed system.

$\vec{n}(\mathbf{r})$ can be expanded in a Taylor series in powers of x, y, z .

Thus

$$n_x(r) = a_1x + a_2y + a_3z + \frac{1}{2}(a_{11}x^2 + a_{22}y^2 + a_{33}z^2 + a_{12}xy + a_{13}xz + a_{23}yz) + \dots$$

$$n_y(r) = a_4x + a_5y + a_6z + \dots$$

and

$$n_z(r) = 1 \tag{5.1}$$

a_1, a_2, \dots are the components of curvature (see Fig. 1.9 in Chapter I).

Considering the apolarity of the director the free energy density of the nematic relative to the free energy density in the state of uniform alignment is given by

$$F_d = \frac{1}{2} \sum_{i,j=1}^6 K_{ij}^{(1)} a_i a_j + \frac{1}{2} \sum_{i,j=1}^6 K_{ij}^{(2)} a_{ij} \tag{5.2}$$

where $K_{ij}^{(1)}$ refer to the coefficients of squares or products of the first derivatives and $K_{ij}^{(2)}$ to the coefficients of the second derivatives. Taking into account the cylindrical symmetry of the medium about \vec{n} the free energy density is given by (Nehring and Saupe 1971)

$$F_d = \frac{1}{2} [K_{11}^{(1)}(S_1 + S_2)^2 + K_{22}^{(1)}(t_1 + t_2)^2 + K_{33}^{(1)}(b_1^2 + b_2^2)] - (K_{22}^{(1)} + K_{24}^{(1)})(S_1 S_2 + t_1 t_2) + K_{13}^{(2)}(d_1 + d_2) \tag{5.3}$$

where

$$\begin{aligned}
 s_1 &= \frac{\partial n_x}{\partial x} , & s_2 &= \frac{\partial n_y}{\partial y} , \\
 t_1 &= -\frac{\partial n_y}{\partial x} , & t_2 &= \frac{\partial n_x}{\partial y} , \\
 b_1 &= \frac{\partial n_x}{\partial z} , & b_2 &= \frac{\partial n_y}{\partial z} , \\
 d_1 &= \frac{\partial^2 n_x}{\partial x \partial z} , & d_2 &= \frac{\partial^2 n_y}{\partial y \partial z} .
 \end{aligned} \tag{5.4}$$

The term associated with $K + K_{24}^{(1)}$ can be expressed as $\text{div}(\vec{n} \text{ div } \vec{n} + \vec{n} \times \text{curl } \vec{n})$ and the term associated with $K_{13}^{(2)}$ can be written as $\text{div}(\vec{n} \text{ div } \vec{n})$. Now terms of the form $\text{div } \vec{u}$ where $\vec{u}(\mathbf{r})$ is an arbitrary vector field may be transformed to surface integrals using the Gauss theorem. These terms do not contribute to the equilibrium condition (Eqn. 1.14) and can thus be omitted when the anchoring at the boundaries is strong. However when the anchoring at the boundaries is weak these terms do contribute to the director configurations and cannot be neglected. The term associated with $(K_{22} + K_{24})$ is zero when only planar configurations are considered (Frank 1958). We are interested only in such deformations and hence this term is omitted in further discussions.

In vector notation the free energy density can then be written as

$$F_d = \frac{1}{2} [K_{11}(\text{div } \vec{n})^2 + K_{22}(\vec{n} \cdot \text{curl } \vec{n})^2 + K_{33}(\vec{n} \times \text{curl } \vec{n})^2] + K_{13}[\text{div } (\vec{n} \text{ div } \vec{n})] \quad (5.5)$$

The elasticity involving K_{13} has also been called the surface like volume elasticity in recent literature (for e.g., Barbero and Strigazzi 1984, Hinov 1987). The importance of K_{13} has been discussed in a few papers. Derzhanski and Hinov (1976) theoretically showed that the formula for determining the flexoelectric coefficient of bending e_3 has to take into account the elastic energy including the second derivatives of the director field. Hinov and Derzhanski (1979) have also shown that K_{13} may lead to a first order Fredericksz transition in homeotropic, planar and twisted nematic layers for some values of the surface energy depending on the sign of K_{13} .

Barnik et al. (1983) studied the director deformations and the corresponding optical characteristics of a nematic liquid crystal MBBA and gave upper and lower limits for K_{13} as $-K_{11/2} \leq K_{13} \leq 0$. Barbero and Strigazzi (1984) have considered the deformations of a hybrid aligned nematic cell which has a planar alignment on one surface and a homeotropic alignment on the other surface. The K_{13} term has been included in the free energy expression. Considering a weak planar alignment and a strong homeotropic alignment the relation $-K_{13} < K_{33/2}$ has been obtained.

Faetti and Palleschi (1985) have used the structural deforma-

tions of a nematic-isotropic interface induced by a magnetic field, to estimate the value of the elastic constant K_{13} at the nematic-isotropic transition temperature. They have incorporated the influence of K_{13} in developing the theory of the deformations of the surface. In their experiment 4-cyano-4'-n-heptyl biphenyl (7CB) was enclosed in a thick cylindrical glass cell of ~ 2 cm height. This was subjected to a vertical temperature gradient in order to obtain a nematic-isotropic interface. A horizontal magnetic field of ~ 7.6 KG was used to align the director in the bulk. The profile of the surface deformations was studied by focussing a laser beam on the interface and monitoring the reflected beam. The final results are affected by a large uncertainty because the physical parameters are known with a poor accuracy at the N-I transition temperature. Accounting for these uncertainties an upper limit for the elastic constant K_{13} has been given as $|K_{13}| < 1.5 \times 10^{-7}$ dynes $- 0.7 K_{33}$ at T_{NI} . However the sign of K_{13} has not been determined by these authors.

We have devised a technique to measure the elastic constant K_{13} in which a hybrid aligned cell is made use of. The director is parallel and strongly anchored at one surface. The other surface is treated for homeotropic alignment with weak anchoring. Consequently, the director makes a small angle θ_0 with the normal to the plate at the second surface (see Fig. 5.1a). The components of \vec{n} are given by $n_x = \sin \theta$, $n_y = 0$ and $n_z = \cos \theta$. An external

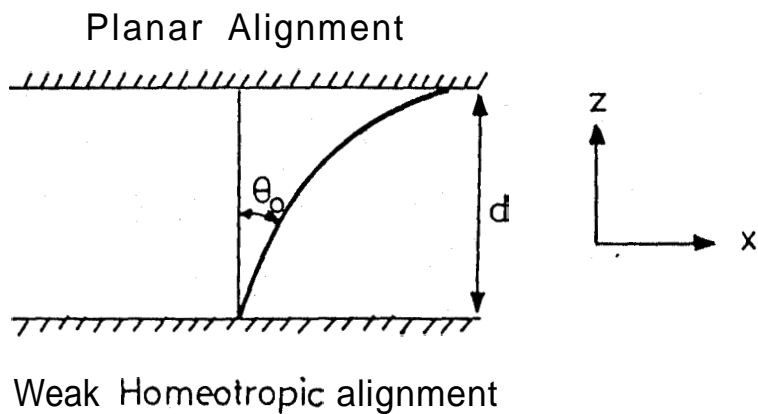
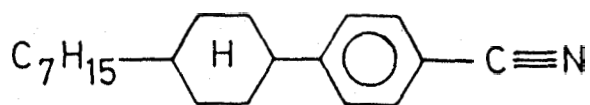


Figure 5.1a

Director profile in the hybrid cell.



p - cyano - p' - heptyl phenyl cyclohexane (PCH-7)

N 56°C I

Figure 5.1b

Structural formula and transition temperature
of PCH-7

magnetic field perpendicular to the plates is used to vary the director profile. The value of θ_0 as a function of the magnetic field strength H can be obtained by an optical technique and the value of K_{13} can be extracted from the surface torque balance equation.

Assuming that θ and $d\theta/dz$ are independent variables at the boundaries also, Oldano and Barbero (1985) have argued that the variational problem does not have a solution corresponding to the K_{13} term. Considering a one constant approximation, i.e., $K_{11} = K_{33} = K$, the free energy is given by

$$F = \frac{1}{2} K \int_0^d \left(\frac{d\theta}{dz} \right)^2 dz + W_0 [\theta(0)] + W_d [\theta(d)] + \frac{1}{2} K_{13} \{ \sin[2\theta(0)] \left(\frac{d\theta}{dz} \right)_0 - \sin[2\theta(d)] \left(\frac{d\theta}{dz} \right)_d \} \quad (5.6)$$

where W_0 and W_d are the surface anchoring energies at $z=0$ and $z=d$ respectively. Oldano and Barbero (1985) now write the first variation of Eqn. (5.6) by taking $\delta\theta(z) = \epsilon\eta(z)$, where ϵ is a small parameter and $\eta(z)$ an arbitrary function. Therefore,

$$\delta F = \epsilon \left[\int_0^d \left\{ -K \left(\frac{d^2\theta}{dz^2} \right) \eta(z) \right\} dz + \left\{ -(K - K_{13} \cos 2\theta) \frac{d\theta}{dz} + \frac{\partial W_0}{\partial \theta} \right\}_0 \eta(0) + \left\{ (K - K_{13} \cos 2\theta) \frac{d\theta}{dz} + \frac{\partial W_d}{\partial \theta} \right\}_d \eta(d) + \frac{1}{2} K_{13} \left\{ \sin(2\theta(0)) \left(\frac{d\eta}{dz} \right)_0 - \sin(2\theta(d)) \left(\frac{d\eta}{dz} \right)_d \right\} \right] \quad (5.7)$$

The requirement that δF be identically zero for any function $\eta(z)$ gives the Euler-Lagrange equation

$$K \frac{d^2 \theta}{dz^2} = 0 \quad (5.8)$$

and the boundary conditions

$$\begin{aligned} - (K - K_{13} \cos 2\theta) \frac{d\theta}{dz} + \frac{\partial W_o}{\partial \theta} &= 0, & z = 0 \\ (K - K_{13} \cos 2\theta) \frac{d\theta}{dz} + \frac{\partial W_d}{\partial \theta} &= 0, & z = d \\ K_{13} \sin 2\theta &= 0, & z = 0 \\ K_{13} \sin 2\theta &= 0, & z = d \end{aligned} \quad (5.9)$$

The general solution of the Euler-Lagrange Eqn. (5.8) depends on only two arbitrary parameters and this solution should satisfy four boundary conditions (Eqn. 5.9). This implies that the problem has no solution in general. In this approximation θ varies discontinuously at the boundaries. This is in contradiction to the basic principles of the continuum theory used in the derivation of the free energy.

Hinov (1987) has argued that θ and $(d\theta/dz)$ and their variations can be considered as dependent functions at the boundaries - the Euler-Lagrange equation and the surface torque balance equation can then be used together to get a continuous solution for θ and the value of K_{13} can be obtained from the surface torque balance equation. Hinov has analysed some theoretical and experi-

mental results obtained on a homeotropic sample of MBBA under the action of an electric field and concluded that the value of the elastic constant K_{13} for MBBA at room temperature has to be slightly smaller than half of the value of the splay elastic constant K_{11} .

As the term associated with K_{13} in Eqn. (5.5) does not contribute to the equilibrium condition for the bulk, viz.,

$$\frac{\partial F_d}{\partial n_\beta} - \frac{\partial}{\partial x_\alpha} \frac{\partial F_d}{\partial g_{\alpha\beta}} = 0$$

where $g_{\alpha\beta} = \partial n_\beta / \partial x_\alpha$, let us first consider the remaining terms in Eqn. (5.5) and write the part of the bulk free energy which contributes to the equilibrium configuration. In the experimental geometry chosen by us there is no twist deformation and the term associated with K_{22} drops out.

$$F_{\text{bulk}} = \int_0^d \left[\frac{K_{11}}{2} \sin^2 \theta \left(\frac{\partial \theta}{\partial z} \right)^2 + \frac{K_{33}}{2} \{ \cos^4 \theta \left(\frac{\partial \theta}{\partial z} \right)^2 + \sin^2 \theta \cos^2 \theta \left(\frac{\partial \theta}{\partial z} \right)^2 \} \right] dz \quad (5.10)$$

where d is, the thickness of the sample. Eqn. (5.10) can be written as

$$F_{\text{bulk}} = \int_0^d \left[\left\{ \frac{K_{11}}{2} \sin^2 \theta + \frac{K_{33}}{2} \cos^2 \theta \right\} \left(\frac{\partial \theta}{\partial z} \right)^2 \right] dz$$

$$= \int_0^d \left[\frac{K_{33}}{2} (1 - \kappa \sin^2 \theta) \left(\frac{\partial \theta}{\partial z} \right)^2 \right] dz \quad (5.11)$$

where $\kappa = (K_{33} - K_{11})/K_{33}$.

In the presence of an applied magnetic field H , Eqn. (5.11) becomes

$$F_{\text{bulk}} = \int_0^d \left\{ \frac{K_{33}}{2} (1 - \kappa \sin^2 \theta) \left(\frac{\partial \theta}{\partial z} \right)^2 - \frac{\Delta \chi H^2}{2} \cos^2 \theta \right\} dz \quad (5.12)$$

where $\Delta \chi$ is the anisotropy of diamagnetic susceptibility per unit volume. Minimising F_{bulk} using the Euler-Lagrange equation

$$K_{33} (1 - \kappa \sin^2 \theta) \left(\frac{\partial \theta}{\partial z} \right)^2 + \Delta \chi H^2 \cos^2 \theta = C \quad (5.13)$$

where C is a constant. This gives

$$\left(\frac{\partial \theta}{\partial z} \right) = \pm \left[\frac{C - \Delta \chi H^2 \cos^2 \theta}{K_{33} (1 - \kappa \sin^2 \theta)} \right]^{1/2} \quad (5.14)$$

Since θ increases with z , the positive root is chosen for $(\partial \theta / \partial z)$ in Eqn. (5.14). The thickness d of the sample

$$d = \int_0^d dz = \int_{\theta_0}^{\pi/2} \frac{d\theta}{\left[\frac{C - \Delta \chi H^2 \cos^2 \theta}{K_{33} (1 - \kappa \sin^2 \theta)} \right]^{1/2}} \quad (5.15)$$

since by definition $\theta = \theta_0$ at $z = 0$ and $\theta = \pi/2$ at $z = d$.

A measurement of the optical path difference introduced by the sample can be used to obtain the variation of θ_0 with applied magnetic field. The incident light beam is polarised at an angle of 45° to the director at the planar aligned surface. If n_o and n_e are the ordinary and extraordinary refractive indices of the

sample, the effective extraordinary refractive index n_{eff} in the sample is given by

$$\frac{1}{n_{\text{eff}}^2} = \frac{\cos^2 \theta}{n_o^2} + \frac{\sin^2 \theta}{n_e^2}$$

or

$$n_{\text{eff}} = n_e n_o / n_e (1 - R \sin^2 \theta)^{1/2} \quad (5.16)$$

where $R = (n_e^2 - n_o^2) / n_e^2$.

The path difference is then given by

$$\begin{aligned} \Delta l &= \int_0^d (n_{\text{eff}} - n_o) dz \\ &= n_o \int_{\theta_o}^{\pi/2} \left[\frac{1}{(1 - R \sin^2 \theta)^{1/2}} - 1 \right] \left(\frac{\partial z}{\partial \theta} \right) d\theta \end{aligned} \quad (5.17)$$

where $(\partial z / \partial \theta)$ is obtained from Eqn. (5.14).

Using known values of n_e , n_o , $\Delta\chi$, K_{11} and K_{33} and our experimentally measured values of the thickness d , path difference Δl and magnetic field H , Eqns. (5.15) and (5.17) can be solved by a suitable iterative procedure to obtain the values of the constant C and θ_o . The corresponding flow chart is given in Fig. 5.2. The value of θ_o thus obtained should also satisfy the surface torque balance equation.

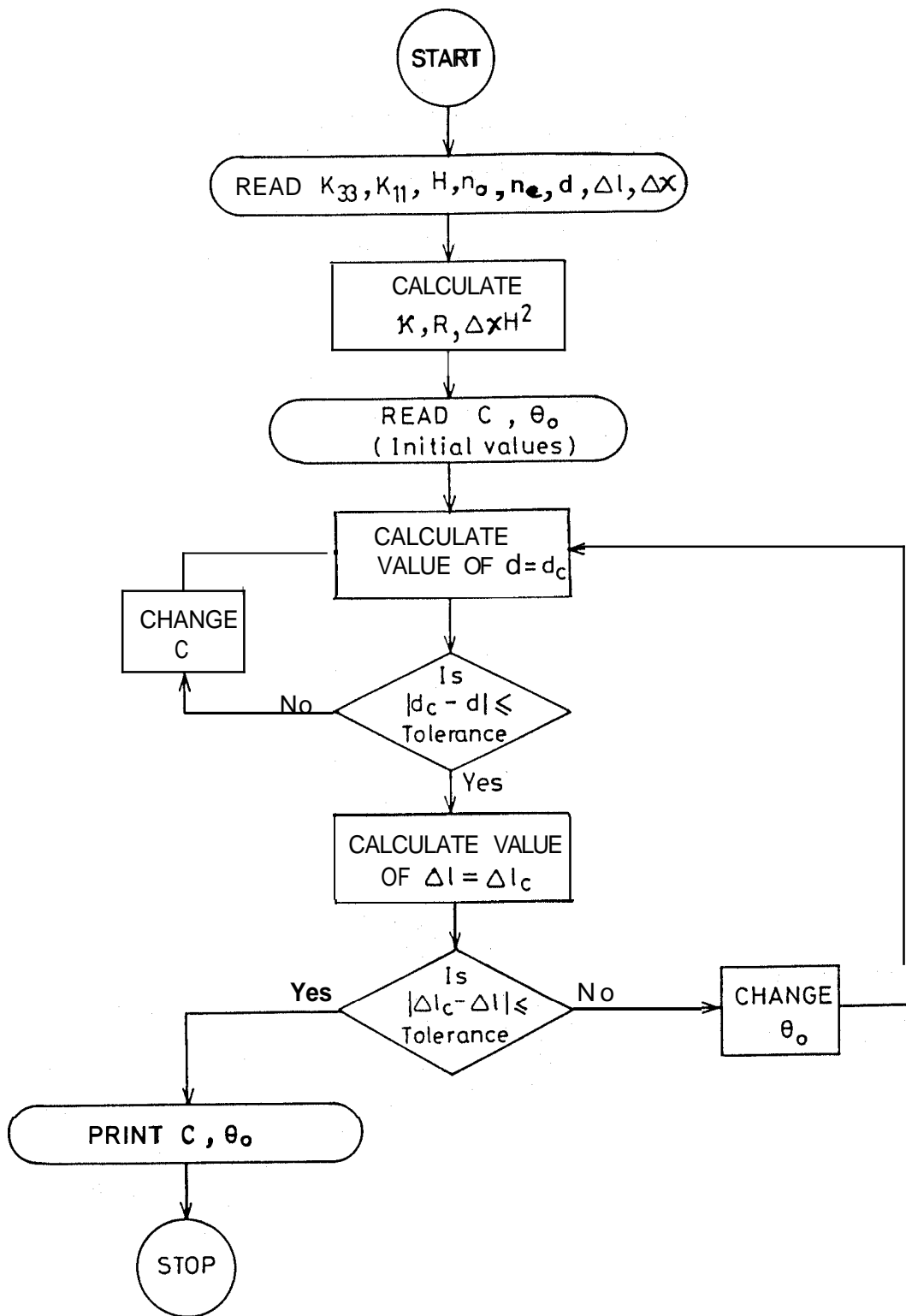


Figure 5.2

Flow chart of the iterative procedure used for the calculation of c and θ_o .

The surface anchoring energy at the weakly anchored surface (i.e., at $z=0$) is assumed to be of the form $\frac{W}{2} \sin^2 \theta_0$ (Vitek and Kleman 1975). The surface torque balance equation at $z=0$ is given by

$$W \sin \theta_0 \cos \theta_0 + K_{13} (\cos^2 \theta_0 - \sin^2 \theta_0) \left(\frac{\partial \theta}{\partial z} \right)_{z=0} \\ + K_{13} \sin \theta_0 \cos \theta_0 \frac{\partial}{\partial \theta_0} \left(\frac{\partial \theta}{\partial z} \right)_{z=0} = K_{33} (1 - \kappa \sin^2 \theta_0) \left(\frac{\partial \theta}{\partial z} \right)_{z=0}$$

Using Eqn. (5.14)

$$W \sin \theta_0 \cos \theta_0 + K_{13} (\cos^2 \theta_0 - \sin^2 \theta_0) \left[\frac{C - \Delta \chi H^2 \cos^2 \theta_0}{K_{33} (1 - \sin^2 \theta_0)} \right]^{1/2} \\ + \frac{K_{13} (\sin 2\theta_0)^2}{4K_{33} (1 - \kappa \sin^2 \theta_0)^2 \left[\frac{C - \Delta \chi H^2 \cos^2 \theta_0}{K_{33} (1 - \kappa \sin^2 \theta_0)} \right]^{1/2}} \{ \kappa C + (1 - \kappa) \Delta \chi H^2 \} \\ = K_{33} (1 - \kappa \sin^2 \theta_0) \left[\frac{C - \Delta \chi H^2 \cos^2 \theta_0}{K_{33} (1 - \kappa \sin^2 \theta_0)} \right]^{1/2} \quad (5.18)$$

The path difference ΔR is measured for the different values of the magnetic field H . Two sets of values of θ_0 and C are obtained by the iterative procedure mentioned before. These are substituted in Eqn. (5.18) to get two equations which can be solved simultaneously to obtain the values of the anchoring energy W and the elastic constant K_{13} .

5.3 THE EXPERIMENTAL METHOD

a) Alignment of the director

The first step in the measurement of the elastic constant K_{13} is the preparation of a suitable hybrid aligned cell. As mentioned before one of the surfaces should have the molecules strongly anchored parallel to the surface. This was achieved by an oblique deposition of SiO on clean glass plates. The other surface should be treated to give a weak homeotropic anchoring. Usually a solution of 0.5% by volume of ODSE (octadecyl triethoxy silane) in methyl alcohol or toluene gives a good homeotropic alignment, with the molecules strongly anchored at the surface. We found that decreasing the percentage of ODSE to 0.05% by volume in methyl alcohol reduces the anchoring strength of p-cyano-p'-heptyl phenyl cyclohexane. It is usually difficult to get a uniform alignment throughout the sample area. We could however select small areas of good alignment for the measurement of the path differences at low temperatures. But as the temperature was increased the alignment deteriorates and the measurements were not possible.

b) Measurement of thickness d of the cell

The thickness of the cell was measured using a double beam ultraviolet spectrophotometer (Hitachi, Model U-3200). Light from the source was allowed to fall normally on the air film between the glass plates. The instrument is programmed to record the values

of A, the wavelength corresponding to the peaks of the interference fringes, over the wavelength range 800 → 500 nm. The thickness is then obtained using the formula

$$t = \frac{n\lambda_1\lambda_n}{2(\lambda_n - \lambda_1)}$$

where λ_1 is the peak value corresponding to the maximum of the first fringe and λ_n to that of the n^{th} fringe. The measurement is made over different areas of the cell. In the calculation of θ_0 , the thickness used corresponds to that of the region over which the path difference is measured. The error in the measurement of the thickness is within $\pm 1\%$.

c) Check for weak anchoring

The actual procedure adopted to obtain θ_0 is tedious and thus before proceeding with the experiment the cell was tested for weak anchoring by making a rough measurement of the path difference. Initially, the path difference per unit thickness of a hybrid cell with strong homeotropic anchoring, at a specific temperature was calculated. For every cell the path difference was measured at the same temperature and compared with the calculated value. A lower measured value of $\Delta\ell$ indicates a non-zero value of the angle θ_0 and hence a weak homeotropic anchoring at the second glass plate. Regions which are free of defects and uniform, and showing the maximum decrease from the calculated value were chosen for further measurements.

d) Temperature control

The cell was mounted in a suitable heater made of copper, to make temperature variations possible (Fig. 5.3). The heater consists of two parts. An outer hollow copper block and a sample holder which can be inserted into the block (see Fig. 5.4). Nichrome wire is wound around the outer copper block which is insulated with sheets of mica. Asbestos powder is packed around the nichrome windings and finally the block is covered with asbestos sheets to minimise heat loss. The sample holder is 'T' shaped and has a slot at the bottom through which the cell can be introduced. Copper screws through the front side of the holder can be tightened to hold the cell in place. There is a circular hole in the sample holder such that a light beam can pass through the sample. The height of the heater can be adjusted such that when the sample holder is inserted into it, the sample area comes exactly at the centre of the pole pieces of an electromagnet (Cook and Sons, Ltd.). The pole-pieces have holes drilled through them for passing the light beam. The applied field was checked for constancy over the field of view using a Gaussmeter with a Hall probe.

The temperature of the heater was varied using a DC power supply (Digireg 233-Digitronics) by suitably varying the applied voltage. The temperature close to the sample was measured using a copper-constantan thermocouple, the hot junction of which is inserted through a hole at the top of the sample holder and is fixed such that it is in contact with the cell.

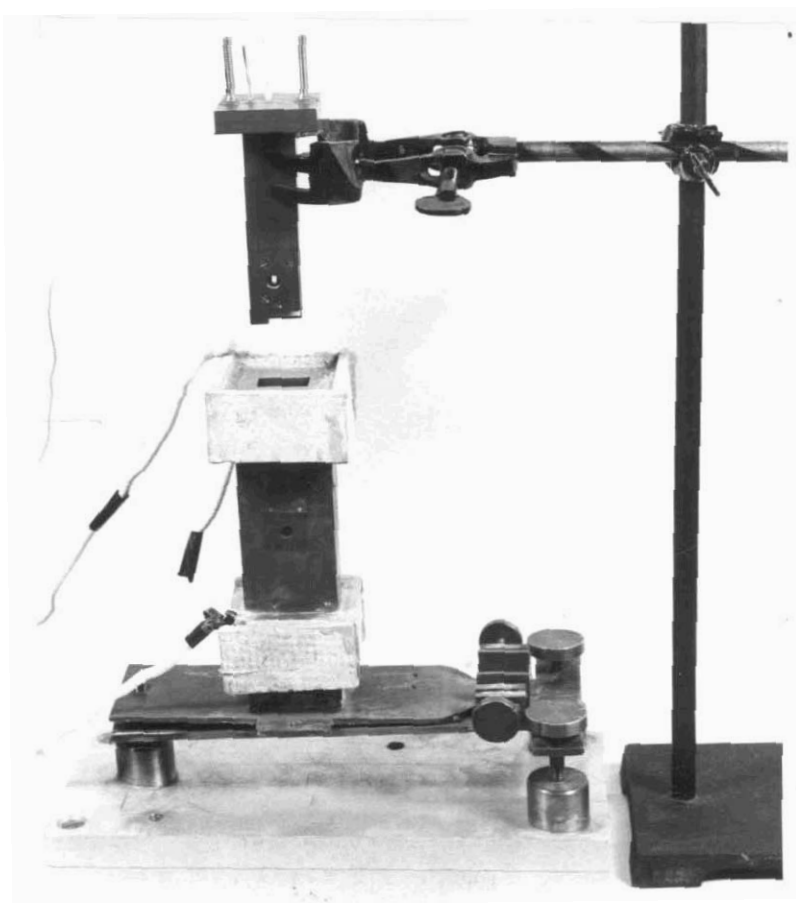


Figure 5.3. Photograph of the heater used in the experimental studies, along with the sample holder.

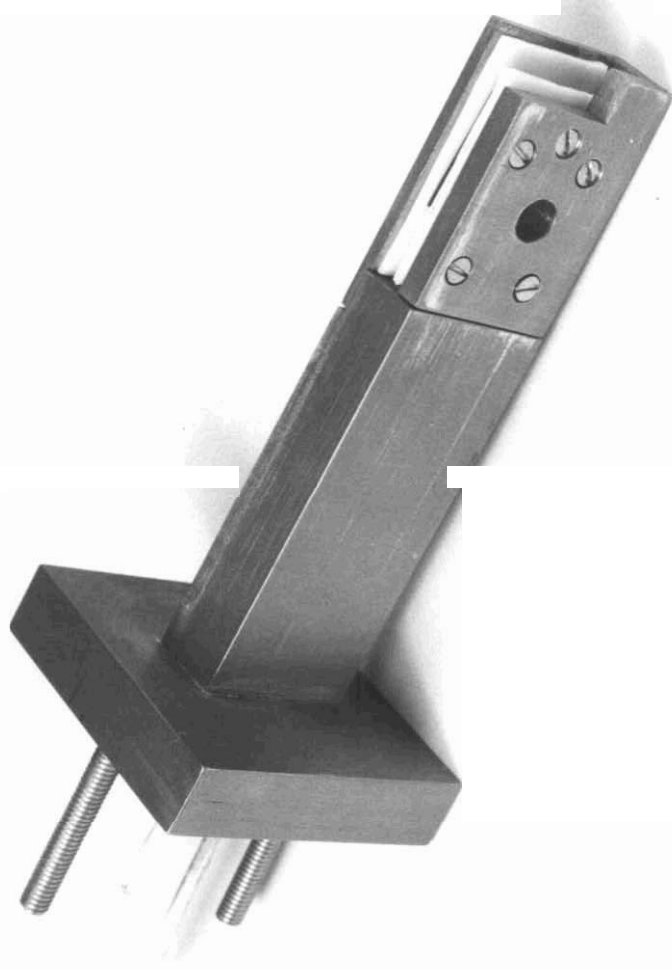


Figure 5.4. Photograph of the sample holder in which the cell mounted.

e) **Calibration of the magnetic field**

The field strength was measured using a Gaussmeter' (Model No. 750 D, RFL Industries Inc.). Before placing the heater at the centre of the pole-pieces, the probe of the Gaussmeter was positioned at the centre and the field strength measured for fixed values of current through the electromagnet.

f) **Path difference measurements**

Optical path difference measurements were made using a tilting compensator (Leitz tilting compensator B) which has a measuring range of about 5λ . The compensator can be inserted into a slot in a frame whose angle can be adjusted suitably. The slow axis of the compensator was adjusted to be perpendicular to the director orientation at the planar surface. The exact compensating band was determined in white light before using monochromatic light. The angle i corresponding to the compensating band can be read off in the window of the drum up to an accuracy of 0.05° . To obtain a result independent of the zero position of the compensator, the compensator plate is tilted in both possible directions during each measurement. The average value is used to obtain the path difference. The compensator works according to the Nikitin-Berek principle. The path differences are calculated using the formula

$$\Delta l = d n_o \left[\left[1 - \frac{\sin^2 i}{n_e^2} \right]^{1/2} - \left[1 - \frac{\sin^2 i}{n_o^2} \right]^{1/2} \right]$$

where d is the thickness of the compensator plate which is -1.52 mm, n_o and n_e are the ordinary and extraordinary refractive indices of the compensator plate which is made of magnesium fluoride. In practice, we make use of a table of path differences, calculated as mentioned, for different values of $2i$ and supplied by Leitz.

In order to increase the sensitivity of measurements, a photo diode was used to detect the exact centre of the compensating band. The signal from this was fed to a lock-in-amplifier (Model 186, Princeton Applied Research Corp.).

The signal from another photo diode on which the direct beam was incident is fed to the reference channel. The best sensitivity range was chosen in the lock-in-amplifier. The approximate value of i corresponding to the centre of the compensating band, i.e., i^* was first obtained by noting the voltage reading on the front panel meter of the lock-in-amplifier as the compensator plate is tilted. The reading initially decreases and then starts increasing. The centre of the band corresponds to the minimum value. More accurate measurements were made by setting the drum of the compensator at specific values and noting the voltage after waiting for 15 min. Beginning from -0.5° of i^* the above procedure was repeated for every 0.05° up to $+0.5^\circ$ of i^* . The voltages obtai-

ned from the panel meter were plotted against the appropriate value of i . The minimum of the curve gives the 'i' value corresponding to the exact centre of the band. The entire procedure was repeated by tilting the compensator plate on the other side and the average value of i was used in the calculation of the path difference.

5.4 THE EXPERIMENTAL SET UP

The actual experimental arrangement is as follows (Fig. 5.5). A sodium vapour lamp is used to obtain monochromatic radiation ($\lambda = 5893 \text{ \AA}$). A glass plate is mounted next to this at 45° to the direction of propagation of the light beam to enable a portion of the beam to be incident on the photo diode, connected to the reference channel of the lock-in-amplifier. A polariser is mounted in the path of the beam. The heater is placed in between the pole pieces of the magnet and the height adjusted by levelling screws present on the base of the heater. A suitable lens system to increase the magnification of the sample is mounted in an aluminium tube which passes through the hole in the pole pieces of the magnet. The tube slot for the compensator is placed next. This is followed by the analyser. After passing through the analyser the light beam is incident on the photo diode connected to the input channel of the lock-in-amplifier. The photo diode is well shielded inside a tube in order to avoid spurious signals.



Figure 5.5. Photograph of the Experimental Set Up.

Initial adjustments

After the sample holder with the cell is inserted into the heater, the polarizer is adjusted to be parallel to the director at the planar aligned surface. The analyser is rotated to get a dark field of view. The sample holder is now removed from the path of the light beam and the tilting compensator is inserted into its slot. Its orientation is adjusted such that the slow axis of the compensator is parallel to the polariser. A black cross oriented at 45° with respect to the polariser is visible in this setting, when the drum reading is zero. The compensator frame is carefully adjusted such that the light beam falls normally on the same. In this case the cross is centred. The frame is then firmly fixed in this position. The polariser and analyser are then rotated by 45° such that they remain crossed.

The sample holder is inserted back into the heater. After stabilising the temperature the path difference is measured at the required value of the applied magnetic field.

5.5 RESULTS AND DISCUSSION

Our experiments were conducted on p-cyano-p'-heptyl phenyl cyclohexane (PCH-7). The structure and transition temperature of which are given in Fig. 5.1b. We found that this compound could be aligned with a weak homeotropic anchoring by the technique

described before. As seen in Eqns. (5.15) and (5.17) we need the following physical parameters for analysing the experimental data, K_{11} , K_{22} and AX which were obtained from the measurements of Schad et al. (1979), the refractive indices n_o and n_e obtained from Pohl et al. (1978) and d , AR and H which were experimentally measured by us as described earlier. The errors in the measurements of K_{33} , K_{11} and $\Delta\chi$ are given to be $\sim \pm 4\%$, $\pm 2\%$ and $\pm 3\%$ respectively. From the plots of n_o and n_e versus temperature given by Pohl et al., we assume that the errors in the measurement is $\sim \pm 0.1\%$ in both. The errors in d and AR are $\sim \pm 1\%$. A significant change in the values of $\Delta\chi$, i.e., in θ_o could be obtained only at field strengths -5000 Gauss. The highest magnetic field that could be obtained with the electromagnet used in the experiment was of the order of 5.6 KGauss. Therefore measurements at more than one value of H could not be made. In the range of -5000 Gauss, H could be measured with an accuracy of $+25$ Gauss. The accuracy of measurements is better at lower temperatures and also the alignment of the sample deteriorates as the temperature is increased. Two independent measurements were made in different cells at temperatures much below the $N-I$ transition temperature. The values of K_{33} , K_{11} , n_o , n_e and $\Delta\chi$ at these temperatures are given in Table 5.1 and the values of K_{13} and W extracted from the Eqn. (5.18) using the iterative procedure described earlier are given in Table 5.2.

TABLE 5.1

$tr = T/T_{NI}$	K_{33} (10^{-5}) dynes	K_{11} (10^{-6}) dynes	n_o	n_e	$\Delta\chi$ (10^{-7}) cgs units
0.9088	0.171	0.99	1.485	1.599	0.346
0.9014	0.177	1.02	1.486	1.601	0.348

TABLE 5.2

$tr = T/T_{NI}$	d (10^{-2}) (cm)	H (Gauss)	$\Delta\lambda$ (10^{-4}) (cm)	K_{13} (10^{-7}) dynes	W (10^{-3}) ergs/cm
0.9088	0.1063	54	0.795	9 ± 4	2.2 ± 0.4
		5480	0.6875		
0.9014	0.1323	54	0.9185	14 ± 4	1.5 ± 0.4
		5440	0.753		

Taking into account the errors in the measurements of the various parameters that figure in the analysis one can estimate that the error in K_{13} is $\pm 4 \times 10^{-7}$ dyne and that in the anchoring energy W is about $\pm 0.4 \times 10^{-3}$ erg/cm (see Table 5.2). The temperatures, at which the two independent measurements were made differ by about 2°C . However since the temperatures are less than $\sim 30^\circ\text{C}$ below the nematic-isotropic transition point, the 2° difference cannot be expected to have a strong influence on K_{13} and the two values agree with each other within the error limits (Table 5.2). At higher temperatures, the alignment of the sample deteriorated and we could not make any measurements.

The sign of K_{13} obtained from the analysis turns out to be positive. Now from the equation for the free energy density (Eqn. 5.5) we see that the elastic constants K_{11} , K_{22} and K_{33} are coefficients of the quadratic terms of the curvature components of \vec{n} and have to be positive in order to give the lowest energy for the undeformed nematic. On the other hand the elastic constant K_{13} is essentially the coefficient of a linear term in the second derivatives of \vec{n} and hence can either be positive or negative. The molecular model of Nehring and Saupe (1972) gives the sign of K_{13} to be negative. In this theory only attractive interactions have been considered and the short range order has been ignored. Further, the shape anisotropy of the molecules has also not been taken into account. But as we discussed in Chapter 3, even the elastic constants K_{11} and K_{33} are strongly affected by short range

order in the medium and these effects can be expected to have a similar influence on K_{13} . Considering the shape factor, deviations from cylindrical symmetry should influence the sign of K_{13} . We can expect that banana shaped molecules should have a positive K_{13} and pear shaped molecules have a negative K_{13} . The compound PCH-7 studied by us has the strongly polar cyano end group (Fig. 5.1b) and hence can be expected to form antiparallel pairs. These pairs can in principle have a banana shaped conformation. This could possibly explain the positive sign of K_{13} found in this compound.

5.6 CONCLUSION

An experimental technique of measuring the elastic constants K_{13} , which requires a weak anchoring of the director at the surface, has been described. An estimate of K_{13} for the nematic liquid crystal p-cyano-p'-heptyl phenyl cyclohexane (PCH-7) has been obtained. The value turns out to be of the same order as the other elastic constants in agreement with dimensional estimates. The sign of K_{13} is found to be positive for this compound. A possible origin for the positive sign has been discussed.

REFERENCES

- Barbero,G., Strigazzi,A. 1984 J. de Phys. Lett., 45, L-857
- Barnik,M.I., Blinov,L.M., Korkishhko,T.V., Umansky, B.A. and Chigrinov,V.G. 1983 Mol. Cryst. Liq. Cryst., 99, 53
- Derzhanski,A.I. and Hinov,H.P. 1976 Phys. Lett., **56A**, 465
- Faetti,S. and Palleschi,V. 1985 J. de Phys., 46, 415
- Frank,F.C. 1958 Disc. Faraday Soc., 25, 19 .
- Hinov,H.P. and Derzhanski,A.I. 1979 J. de Phys., 40, C3-505
- Hinov,H.P. 1987 Mol. Cryst. Liq. Cryst., 148, 197
- Madhusudana,N.V. and Durand,G. 1985 J. de Phys. Lett., 46, L-195 (1985)
- Nehring,J. and Saupe,A. 1971 J. Chem. Phys., 54, 337
- Nehring,J. and Saupe,A. 1972 J. Chem. Phys., 56, 5527
- Oldano,C. and Barbero,G. 1985 Phys. Lett., **110A**, 213
- Oseen,C.W. 1933 Trans. Faraday Soc., 29, 883
- Pohl,L., Eidenschink,R., Krause,J. and Weler,G. 1978 Phys. Lett., **65A**, 169
- Schad,H., Baur,G. and Meier,G. 1979 J. Chem. Phys., 70, 2770
- Vitek,V. and Kleman,M. 1975 J. de Phys., 36, 59